九州大学大学院総合理工学報告
第30巻　第4号　406-411頁　平成21年3月

Engineering Sciences Reports, Kyushu University
Vol. 30, No. 4, pp. 405-410, MAR. 2009

Evaluation of Heat of Adsorption of Methane, R507A and HFC-134a from Desorption Method

Khairul HABIB*1 Bidyut Baran SAHA*2,†
Ibrahim Ibrahim El-SHARKAWY*2 and Shigeru KOYAMA*2
†E-mail of corresponding author: *bidyutb@cm.kyushu-u.ac.jp*

(Received February 5, 2009)

This article deals with the evaluation of isosteric heat of adsorptions from adsorption of methane, R507A and HFC-134a on highly porous activated carbon of type Maxsorb III by desorption method The adsorption isotherms and heat of adsorption of methane, R507A and HFC-134a on the assorted adsorbent are measured experimentally over a temperature ranging from 5 to 70˚C. The pressure variations for methane + Maxsorb III and HFC-134a + Maxsorb III systems are from 2 to 20 bar. However, for R507A + Maxsorb III system the pressures are being varied from 2 to 13 bar. The heat of adsorption data are useful in designing adsorption cooling and storage systems.

Key words: *Isosteric heat of adsorption, Maxsorb III, Methane, R507A, HFC-134a*

1. Introduction

The isosteric heat of adsorption (Q_{st}) is a specific combined property of an adsorbate + adsorbent combination. It is one of the key thermodynamic variables for the design of practical gas storage systems[1-2] and adsorption cooling systems[3-7]. It determines the extents of adsorbent temperature changes within the adsorber during adsorption (exothermic) and desorption (endothermic) steps of the precesses. The adsorbent temperature is a key variable in evaluating the local adsorption equilibria and kinetics on the adsorbent, which ultimately govern the seperation performance of the precesses.

Several researchers have measured the physical adsorption of methane on activated carbon[8-12]. Methane is the main ingredient of natural gas and it has an advantage as a dominant fossil fuel over other gases as it plays a vital role in maintaining a clean environment. It remains clean during burning and after burning no ash partiles are left. Natural gas has a relatively lower emissions of sulphur, carbon and nitrogen. In the transport sector, adsorbed natural gas can be used more effectively than compressed natural gas (CNG). Because the operating pressure is very high for CNG which results in higher costs. But, ANG can operate at significantly lower pressure, which can contribute substantially in the reduction of gas storage cylinder cost. The isosteric heat of adsorption of methane into activated carbon is one of the key factors of the performance of the ANG.

The refrigerant R507A is an azeotropic blend consisting of 50% R125 (pentafluoroethane) and 50% R143a (1,1,1−trifluoroethane) by weight. The use of chlorofluorocarbons (CFCs) has been substantially reduced after the Montreal protocol. The refrigerants R125 and R143a are hydrofluorocarbons (HFCs) and they do not contribute to the stratospheric ozone layer. It has relatively smaller global warming potential (GWP) compared with the CFCs and the ozone depletion potential (ODP) is zero. It is also non-flammable and the level of acidity is significantly small (below 1.0 ppm). Adsorption of R507A on activated carbon has been carried out by the authors of the present study[13-14].

HFC-134a (1,1,1,2−tetrafluoroethane) has been introduced for the purpose of refrigeration in order to protect stratospheric ozone layer. Adsorption cycle is consisdered as one of the most promising environmental−friendly cooling systems as

*1 Department of Energy and Environmental Engineering, Graduate student
*2 Department of Energy and Environmental Engineering

these systems can be powered by low-temperature thermal heat and can utilize HFC based refrigerant. As a consequence, several researches have been carried out adsorption experiments of HFC-134a on various activated carbons[15-18].
The present paper evaluates isosteric heat of adsorption of methane, R507A and HFC-134a on Maxsorb III. Desorption method has been used to measure adsorption isotherms and heat of adsorption data of all three assorted adsorbate + adsorbent pairs.

2. Experimental

2.1 Materials

The pitch based activated carbon (Maxsorb III specimen) labeled as MSC-30 has been supplied by the Kansai Coke and Chemical Co. Ltd., Japan. It has a Brunauer–Emmet–Teller (BET) surface area of 3,140 m^2/g and micropore volume of 1.7 cc/g. The mean particle diameter of Maxsorb-III specimen is 72 μm, ash content is less than 0.1%, moisture of no more than 0.8% and pH value is 4.1.

2.2 Experimental setup

The schematic diagram of the experimental test rig is shown in Figure 1, which comprises a mass flow regulator (Kojima-Kofloc-5100), a pressure transducer (Kyowa-PGS-50KA), several K type thermocouples (Chromel–Alumel) and a data acquisition system (Keithtly 2700). A water circulating bath (TBN302DA) is used to control the flow and temperature of water and it has a stability within ±0.1°C. To stop the migration of the activated carbon during evacuation and desorption, a filter of 2 micron stainless steel fine mesh was fitted in the plumb line at the exit of the adsorption cell.
The Maxsorb III specimen that has a mass of 65.66 g and net packing density of 0.31 g/cc is kept inside a cylindrical shaped adsorption cell. The internal diameter of the cylinder is 30 mm with a depth of 300 mm and volume of 212 cm^3. The cell is designed to tolerate pressure up to 50 bar at a temperature of 150°C. The external plumbing is made of nominal stainless steel having thickness (t) of 0.635 mm and inner diameter of 4.35 mm, and the total volume of the internal plumbing is estimated to be 13.1 cc. All valves are of Swagelok SS 304 type. Detail description of the experimental setup can be found elsewhere[8].

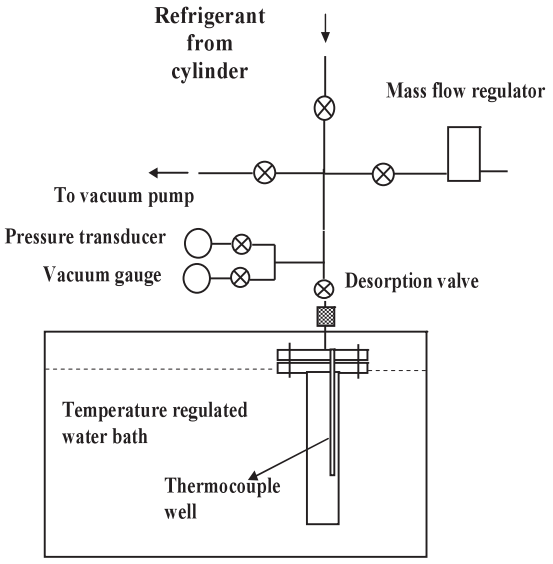

Fig. 1 Schematic diagram of the experimental test rig.

2.3 Experimental procedure

Prior to each experiment, the adsorption cell was subjected to repeated filling and evacuation sequences. This is to ensure that the remaining gas is only the assorted adsorbate. During experiment, the adsorbate is charged slowly into the adsorption cell at a temperature of 5-10°C, which is defined as the adsorption temperature (T_a). When equilibrium attains, the temperature of the adsorption cell is raised isosterically to the desired temperature. As a result, both pressure and temperature are increased and these pressure and temperature data are collected to obtain isosteric heat of adsorption. When the cell achieves equilibrium at the desired temperature, the pressure at that point is referred as initial pressure (p_i) which is followed by desorption. The cell is then gradually desorbed over periods of the order of several 100's of seconds until the flow rate falls to a value that is one order magnitude higher than the uncertainty of the mass flow regulator used in the present study.
The pressure of the adsorption cell is allowed to stabilize at state 3 which gives the final pressure after the completion of desorption on the isotherm (p_f). For methane, experiments were conducted at temperatures and pressures which are higher than critical

temperature and pressure of methane. But for HFC-134a and R507A, the charging pressure is always lower than the saturation pressure corresponding to the temperature of the adsorption cell to ensure that no condensation is occurred.

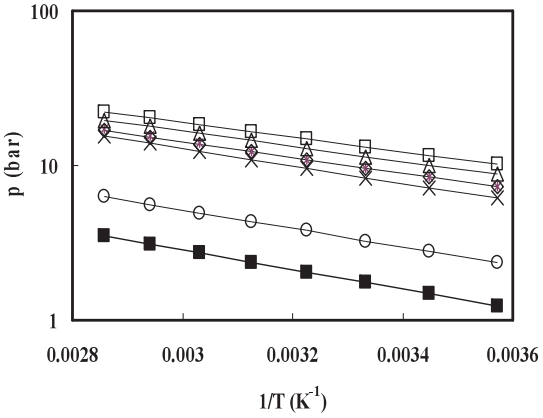

Fig. 2 Plot of lnP vs $1/T$ at different concentrations (C/C_0) Legends: ■-0.059 and 0.086, O-0.11, X-0.23, ◊- 0.26, □-0.33, □ - 0.35.

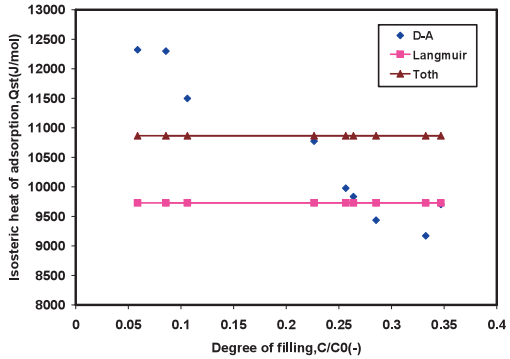

Fig. 3 Isosteric heat of adsorption varying with concentration.

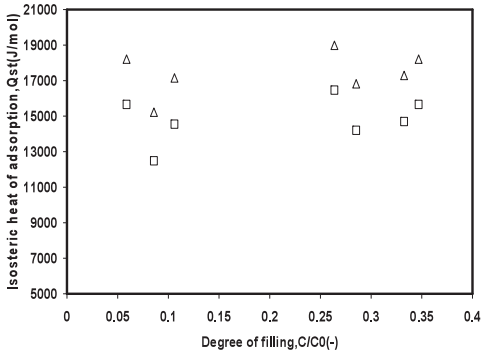

Fig. 4 Isosteric heat of adsorption against surface coverage for adsorption of methane □n Maxsorb III;( ):experimental data points; (Δ):

2.4 Data reduction

The primary data of flow rate, cell and ambient temperatures and pressure are time dependent. Details of data reduction has also been explained elsewhere[8].

3. Theoretical analysis

3.1 Heat of adsorption

The isosteric heat of adsorption, Q_{st} is defined as the differential change in energy (δQ) that occurs when an infinitesimal amount of adsorbates (δm_a) are transferred at constant pressure, P, temperature, T and pore surfaces or mass of adsorbent, M_s from the bulk gas phase (g) to the adsorbed phase (a) and can be written as[19],

$$Q_{st} = \left(\frac{\partial Q}{\partial m_a} \right)_{P,T,M_s} \tag{1}$$

Heat of adsorption (Q_{st}), which is a function of concentration, has a weak dependence on temperature[15-20]. Clausius-Clapeyron (C-C) equation is generally used to estimate heat of adsorption at constant concentration,

$$Q_{st} = -R \frac{\partial \ln P}{\partial \left(\frac{1}{T} \right)} \tag{2}$$

where, R is the universal gas constant in J/kg-K.

From experimental results, Q_{st} could be classified according to the three distinctive behaviors for a variety of micro and mesoporous adsorbents: (i) an energetically homogeneous adsorbent, when exposed to certain type of adsorbate, would exhibit a constant Q_{st} with increasing adsorbate uptake, (ii) the Q_{st} may decrease with increasing adsorbate uptake due to the variability in the energetic heterogeneity, and (iii) the Q_{st} may also increase with increasing adsorbate loading, which is caused by the stronger lateral interactions between the adsorbed molecules at higher surface coverage.

In the present study, heat of adsorption, Q_{st} as a function of adsorbate vapor uptake is calculated from the measured adsorption isotherm by the following experimentally

validated correlation and can be expressed as[19],

$$Q_{st} = Q_{st}\big|_{C-C} + Tv_g \left.\frac{dP}{dT}\right|_{gas} \qquad (3)$$

where the first term of the right hand side of eq. 3 represents the general form of heat of adsorption and the second term indicates the behavior of adsorbed mass with respect to both pressure and temperature changes during an adsorbate uptake, which occurs due to the non-ideality of gaseous phase. In eq. 3, v_g is the specific volume of the vapour phase and dp/dT defines the gradient of the pressure with temperature of the adsorbate.

3.2 Adsorption isotherms

In this study, experimental data of methane and R507A are fitted with Dubinin-Astakhov (D-A), Langmuir and Tóth isotherm models, while R134a data are fitted with D-A model only. D-A, Langmuir and Tóth isotherm models can be written as,

$$W = W_o \exp\left[-\left\{\frac{RT}{E}\ln\left(p_s/p\right)\right\}^n\right] \qquad (4)$$

where $W = Cv_a$, with v_a being the adsorbed phase volume.

$$\frac{C}{C_o} = \frac{k_0 \exp\left(Q_{st}/RT\right) p}{1 + k_0 \exp\left(Q_{st}/RT\right) p} \qquad (5)$$

$$\frac{C}{C_0} = \frac{k_0 \exp\left(Q_{st}/RT\right) p}{\left[1 + \left\{k_0 \exp\left(Q_{st}/RT\right)\right\}^t\right]^{\frac{1}{t}}} \qquad (6)$$

One form of Tóth equation used for methane experiments can be written as[8],

$$\frac{C}{C_0} = \frac{P}{\left[\dfrac{k_0\sqrt{MT}}{\exp\left(\dfrac{Q_{st}}{RT}\right)} + P^t\right]^{1/t}} \qquad (7)$$

The experiments of methane are performed in the super critical range, so we have used a pseudo-relation to obtain the saturation pressure, p_s at the desired desorption temperature [21],

$$p_s = \left(\frac{T}{T_c}\right)^2 p_c \qquad (8)$$

For HFC-134a, T_b = 246.78K, T_c = 374.21K, V_b = 7.2643x10^{-4} m^3/kg and Van der Waals volume $b = RT_c/8P_c$, P_c for HFC-134a is 40.59 bar, yieling b = 9.39x10^{-4} m^3/kg. The saturation vapor pressure is calculated from the NIST database.
For R507A, T_c = 343.8K, T_b = 226.4K, V_b = 7.59x10^{-4} m^3/kg, b = 9.75x10^{-4} m^3/kg. The saturation vapor pressure is also calculated from the NIST database.

4. Results and Discussion

Fig. 2 shows the $ln(p)$ versus $1/T$ plot for calculating the isosteric heat of adsorption. These plots are generated from slopes and intercepts of experimental data on pressure and temperature. As can be seen from Fig. 2, all experimental data can be represented by straight lines with regression coefficient above 99.9%. The slopes define the value of $-Q_{st}/R$.
The effect of isosteric heat of adsorption on adsorbate (methane) uptake is shown in Fig. 3. It is found from Fig. 3 that using Langmuir and Tóth models, one can observe the straight line behavior of isosteric heat of adsorption for methane uptake on to Maxsorb III, which indicates the average value of isosteric heat of adsorption. It is also observed from the Fig. 5 that the isosteric heat of adsorption decreases with increasing adsorbate (methane) when D-A model is applied. The assorted adsorbent (Maxsorb-III) consists mainly of micropores with different width and methane adsorbs rapidly on to the sites of high energy, and as adsorption progresses, molecules adsorb onto sites of decreasing energy. The methane molecules first penetrate into narrower pores of Maxorb-III, resulting in a stronger interaction between methane and Maxsorb-III. This implies a higher value of isosteric heat of adsorption at lower loading. After completely filling the smaller pores, methane molecules are gradually accommodated in relatively larger pores, in which the adsorption affinity becomes weaker. Therefore, a monotonic decrease in isosteric

heat of adsorption as a function of adsorbate (methane) uptake is observed in Fig. 3.

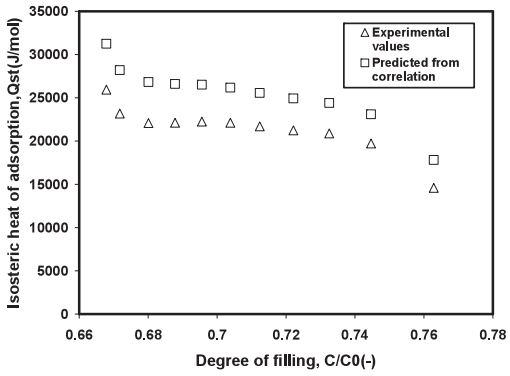

Fig. 5 Isosteric heat of adsorption against adsorbate uptake for adsorption of R507A on Maxsorb III.

A satisfactory agreement between the present experiments and correlation proposed by Chakraborty et al.[19] is shown in Fig. 4. The experimental results have been calculated by Clausius-Clapeyron equation.

Fig. 5 depicts isosteric heat of adsorption against surface coverage of R507A between experimental data and the correlation of Chakraborty et al.[19]. From Fig. 5, it is noticeable that the values predicted from the Chakraborty et al.[19] are slightly higher than the experimentally calculated ones. The reason for this behavior is that Chakraborty et al.[19] assumed an extra term of non-ideality of gas phase added with the conventional form of Clausius-Clapeyron equation.

Fig. 6 shows the plot of lnP vs $1/T$ for adsorption of HFC-134a on Maxsorb III for different concentrations. The slope of the tangent yields $-Qst/R$.

For adsorption of HFC-134a on Maxsorb III, the effects of isosteric heat of adsorption on surface loading are shown in Fig. 7. It can be observed from Fig. 7 that the values of isosteric heat of adsorption evaluated from the experiments are very close with the values of correlation predicted by Chaktaborty et al.[19].

4. Conclusions

Isosteric heat of adsorption has been evaluated from the adsorption of methane, R507A and HFC-134a on to maxsorb III through desorption measurements. Dubinin-Astakhov (D-A) isotherm model founds to be most suitable to represent all the experimental data. The isosteric heat of adsorption data evaluted in the present paper are useful in designing adsorption cooling and gas storage systems.

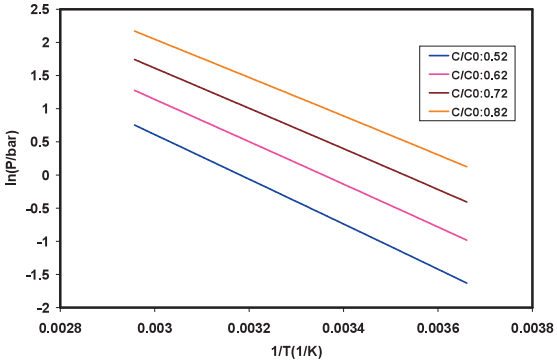

Fig. 6 Plot of lnP vs $1/T$ for adsorption of HFC-134a on Maxsorb III.

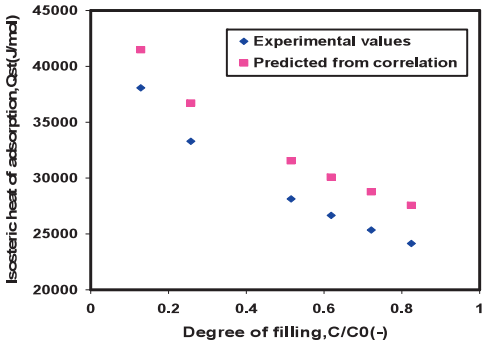

Fig. 7 Isosteric heat of adsorption against surface coverage for adsorption of HFC-134a on Maxsorb III.

Nomenclature

M_s	mass of adsorbent	kg
m_a	mass of adsorbate	kg
Q	power	W
Q_{st}	isosteric heat of adsorption	J/mol
R	universal gas constant	J/kg·K
p	pressure	bar
p_s	saturation pressure	bar
T	temperature	K
W	volumetric uptake	m^3/kg
W_0	limiting volumetric uptake	m^3/kg
C	adsorption uptake	kg/kg
C_0	limiting uptake	kg/kg
E	characteristic energy	J/mol
n	heterogeneity constant	-
t	Tóth constant	-
M	molecular weight	kg/kmol
v	volume	m^3/kg

Subscripts

g　gaseous phase

References

1) C. Liu et al.,Appl. Phys. Lett., 80 (2002) 2389.
2) A.N. Fedorov et al., Gas Sep. Purif., 9 (1995) 137.
3) B.B. Saha et al., Int. J. Refrigeration, 26 (2009) 749.
4) B.B. Saha et al., Philos. Mag., 86(2) (2006) 613.
5) B.B. Saha et al., Int. J. Refrigeration,30(1) (2007) 86.
6) B.B. Saha et al., Int. J. Refrigeration,30(1) (2007) 96.
7) K.Habib et al., Proc. 10th Cross Straits Symp., Japan November 13-14, 2008.
8) B.B. Saha et al., J. Chem. Engg. Data, 52(6) (2007) 2419.
9) K.Habib et al., Eng. Scien. Reports, Kyushu Univ., 29(2) (2007) 300.
10) F.N. Ridha et al., Fuel Process. Tech., 88 (2007) 349.
11) Y. Zhou et al., Carbon, 43 (2005) 2007.
12) M. Bastos-Neto et al., Adsorption, 11 (2005) 911.
13) B.B. Saha et al., J. Chem. Engg. Data, 53(8) (2008) 1872.
14) K. Habib et al., Proc. 9th Cross Straits Symp., Korea November 21-22, 2007.
15) B.S. Akkimaradi et al., J. Chem. Engg. Data, 46 (2001) 417.
16) S. Savitz et al., J. Phys. Chem. B, 103 (1999) 8283.
17) S.H. Lin et al., J. Environ. Eng., 125(11) (1999) 1048.
18) N.D. Banker et al., Carbon, 42 (2004) 117.
19) Chakraborty et al., Appl. Phys. Lett., 89 (2006) 171901.
20) M. Prasad et al., Carbon, 37 (1999) 1641.
21) S. Ozawa et al., J. Coll. Inter. Sci., 56(1) (1976) 83.